Tazzoliite: a new mineral with a pyrochlore-related structure from the Euganei hills, Padova, Italy

Cámara F; Nestola F; Bindi L; Guastoni A; Zorzi F; Peruzzo L; Pedron D. Tazzoliite: a new mineral with a pyrochlore-related structure from the Euganei hills, Padova, Italy. MINERALOGICAL MAGAZINE. 76 pp: 827-838.
DOI: 10.1180/minmag.2012.076.4.01

Revision 1

Tazzoliite: a new mineral with a pyrochlore-related structure from Euganei hills, Padova, Italy

F. Cámara[1]*, F. Nestola[2], L. Bindi[3], A. Guastoni[4], F. Zorzi[2], L. Peruzzo[5], D. Pedron[6]

[1]Dipartimento di Scienze della Terra, Università di Torino, Via Valperga Caluso 35, I-10125 Torino, Italy; *e-mail: fernando.camaraartigas@unito.it

[2]Dipartimento di Geoscienze, Università di Padova, Via Gradenigo 6, I-35131 Padova, Italy

[3]Dipartimento di Scienze della Terra, Università di Firenze, Via La Pira 4, I-50121 Firenze, Italy

[4]Museo di Mineralogia, Università di Padova, Via Giotto 1, I-35122 Padova, Italy

[5]C.N.R., Istituto di Geoscienze e Georisorse, Via Gradenigo 6, I-35131 Padova, Italy

[6]Dipartimento di Scienze Chimiche, Università di Padova, Via Marzolo 1, I-35131 Padova, Italy

Abstract

Tazzoliite, ideally $Ba_2CaSr_{0.5}Na_{0.5}Ti_2Nb_3SiO_{17}[PO_2(OH)_2]_{0.5}$, is a new mineral (IMA 2011-018) found at Monte delle Basse, Euganei Hills, Galzignano Terme, Padova, Italy. It occurs as lamellar, light-orange crystals up to 0.3-0.4 mm in length and only a few μm in thickness, closely associated with a diopsidic pyroxene and titanite. Tazzoliite crystals are transparent, have a white streak and pearly lustre. It is not fluorescent and has a hardness of 6 (Mohs scale). The tenacity is brittle and crystals have a perfect cleavage along {010}. The calculated density is 4.517 g/cm^3. Tazzoliite is biaxial (-) with a 2*V* of about 50°; it does not show pleochroism and the average refractive index is 2.04. No twinning was observed. Electron-microprobe analyses gave the following chemical formula:

$(Ba_{1.93}Ca_{1.20}Sr_{0.52}Na_{0.25}Fe^{2+}_{0.10})_{\Sigma 4}(Nb_{2.88}Ti_{2.05}Ta_{0.07}Zr_{0.01}V^{5+}_{0.01})_{\Sigma 5.02}SiO_{17}$ $[(P_{0.13}Si_{0.12}S_{0.07})O_{0.66}(OH)_{0.66}][F_{0.09}(OH)_{0.23}]_{\Sigma 0.32}$.

Tazzoliite is orthorhombic, space group *Fmmm*, with unit-cell parameters: a = 7.4116(3) Å, b = 20.0632(8) Å, c = 21.4402(8) Å, V = 3188.2(2) Å^3 and Z = 8. The crystal structure, obtained by single-crystal X-ray diffraction data, was refined up to $R_1(F^2)$ = 0.063. It consists of a framework of Nb(Ti)-octahedra and BaO_7 polyhedra sharing apexes or edges, and Si-tetrahedra sharing apexes with Nb(Ti)-octahedra and BaO_7 polyhedra. The structure, which is related to the pyrochlore structure, is constituted by three Nb(Ti)-octahedra, two of them are Nb and Ti dominant, respectively. Chains of $A2O_8$ polyhedra [$A2$ being occupied by Sr(Ca, Fe)] extend along [100] and are surrounded by Nb-octahedra. Channels formed by six Nb(Ti)-octahedra and two tetrahedra, or four $A1O_8$(OH) polyhedra ($A1$ being occupied by Ba), alternate along [100]. The channels are partially occupied by $[PO_2(OH)_2]$ in two possible mutually exclusive positions, alternating with fully occupied $A3O_7$ polyhedral pairs [$A3$ being occupied by Ca(Na)]. The eight strongest X-ray powder-diffraction lines [d in Å (I/I_0) (hkl)] are: 3.66 (60) (044), 3.16 (30) (153), 3.05 (100) (204), 2.98 (25) (240), 2.84 (50) (004), 2.72 (20) (155), 1.85 (25) (400) and 1.82 (25) (268). Raman spectra of tazzoliite were collected in the range 150-3700 cm^{-1} and confirm the presence of (OH) groups. Tazzoliite is named after Vittorio Tazzoli in recognition of his contribution to the fields of mineralogy and crystallography.

Key-words: tazzoliite, new mineral, crystal structure, pyrochlore, Raman spectroscopy, Euganei Hills.

Introduction

The new mineral tazzoliite, here described, was found in the vicinity of Monte delle Basse at the Euganei Hills, south of Galzignano Terme, Padova, Italy (45° 18’ 30” N − 43° 49’ 47” E) by mineral collector Mr. Bruno Fassina. The geology is characterised by lower Oligocene rhyolites and trachytes (Figure 1). In the area of tazzoliite finding also scarce syenitic and gabbroic rocks are present, which, based on an old hypothesis, would represent the deep segregation products of rhyolitic and trachytic magmas (Dal Piaz, 1935). Skarn and calcsilicate rocks can also be observed in contact with the intrusives (Stark, 1936). These rocks are comprised of wollastonite, garnet (grossular), gehlenite, sanidine, gyrolite, hibschite, kilchoanite, pectolite, rankinite and plagioclase, and rarely sanidine xenoliths rich in vugs up to several millimeters across. Inside these vugs tazzoliite was found as fan-shaped groups of platy crystals (Figure 2), light-orange in colour, up to 0.3-0.4 mm in length and only a few μm in thickness.

Tazzoliite was approved by the IMA-Commission on New Minerals, Nomenclature and Classification (IMA 2011-018). The name is in honour of Professor Vittorio Tazzoli (b. 1938) in recognition of his contribution to the fields of mineralogy and crystallography, particularly in the area of pyroxenes. He has contributed to the structure solution of numerous minerals. Type material is deposited in the collections of the Museo di Mineralogia di Padova, Italy, registration number MMP M9426.

Association and physical properties

Tazzoliite is associated with a green diopsidic pyroxene and titanite. It is light-orange in colour. It shows a white streak; the lustre is pearly and crystals are transparent. It is not fluorescent and has a hardness of 6 on the Mohs scale (VHN load 15g, mean 788 kg

mm^{-2}). The tenacity is brittle and crystals have a perfect cleavage along {010}. No parting was observed and the fracture is uneven.

Optically, tazzoliite is biaxial (-), and based on the Gladstone-Dale method (Mandarino, 1976) the calculated average refractive index is 2.04. The 2*V* (meas.) is 50(5)° and no pleochroism was observed. No twinning was detected.

Experimental methods

Microprobe analysis

Microprobe analyses (7 WDS spots) were obtained on the same crystal fragment used for the structural study using a CAMECA SX-50 electron microprobe. Operating conditions were 20 kV and 20 nA, spot size 2 μm, for Si, Ti, V, Nb, Ta, Fe, Mn, Sn, Zr, Ca, Ba, and 20 kV and 10 nA, spot size 10 μm for F, Na, P, S, Sr. The second scheme was adopted to avoid beam damage. The crystal was found to be homogeneous within analytical uncertainty. H_2O was calculated and checked on the basis of the structure refinement. K, Cr and Cl were not detected. REE were sought for but were below detection limit. Analytical data are given in Table 1. The empirical formula is calculated by iterative process on the basis of (18 + 2*x*) (O,F) *apfu* with *x* = [P + S + (Si-1)] < 0.5 *apfu*, to take into account partial occupancy of anionic groups at the channels (see crystal structure description). We obtain $(Ba_{1.93}Ca_{1.20}Sr_{0.52}Na_{0.25}Fe^{2+}_{0.10})_{\Sigma 4}(Nb_{2.88}Ti_{2.05}Ta_{0.07}Zr_{0.01}V^{5+}_{0.01})_{\Sigma 5.02}SiO_{17}[(P_{0.13}Si_{0.12}S_{0.07})O_{0.66}(OH)_{0.66}][F_{0.09}(OH)_{0.23}]_{\Sigma 0.32}$.

X-ray diffraction

A single crystal of tazzoliite (0.100 × 0.040 × 0.015 mm^3), inclusion- and twinning-free with sharp optical extinction and sharp reflections, was selected for the X-ray

diffraction analysis. The sample was measured using a Bruker AXS single-crystal diffractometer equipped with a CCD Smart APEX detector and Mo*K*α graphite-monochromatized radiation. Images were collected with an ω increment of 0.2°. Cell parameters were refined using 5584 reflections with $I/\sigma(I) > 10$. A total of 12200 reflections were collected in the 2θ range 3.8-60.0°, of which 1312 were unique (R_{int} = 5.4%); absorption and Lp correction were applied. The structure was solved using Superflip software (Palatinus and Chapuis, 2007). Weighted full-matrix least-squares refinement on F^2 was performed using SHELX97 (Sheldrick, 2008). Crystal data are reported in Table 2 whereas the calculated X-ray powder diffraction pattern (114.6 mm diameter Gandolfi camera - Cu*K*α) is given in Table 3. Final atom positions and displacement parameters are listed in Table 4 and bond lengths in Table 5.

Unit cell parameters refined from powder data are as follows: a = 7.4116(3) Å, b = 20.0632(8) Å, c = 21.4402(8) Å, and V = 3188.2(2) Å^3.

Raman spectroscopy

Raman spectra were collected with a home-built micro-Raman system, based on a single 320 mm focal length imaging spectrograph, a Triax-320 ISA instrument, equipped with a holographic 1800 g/mm grating and a liquid-nitrogen-cooled CCD detector (Spectrum One ISA Instruments). The excitation source was a Spectra Physics Ar laser (Stabilite 2017-06S) operating at 514.5 nm. A Kaiser Optical System holographic notch filter (514.5 nm) was used to reduce the stray-light level. An Olympus BX 40 optical microscope equipped with three objectives, 20×/0.35, 50×/0.75, and 100×/0.90, was optically coupled to the spectrograph. This made it possible to observe the sample with the microscope and then to select particular micrometric regions for Raman analysis. With the 100× objective, the lateral

resolution is estimated to be 0.5 μm and the depth of focus 1–2 μm. To avoid optical damage to the sample, the power of the exciting radiation was maintained between 10 and 50 mW. Raman spectra were recorded between 147 and 4000 cm^{-1} with an instrumental resolution of about 2 cm^{-1}.

Results and discussion

Crystal structure

Tazzoliite is orthorhombic, space group *Fmmm*, with the following unit-cell parameters: a = 7.4105(4) Å, b = 20.0675(11) Å, c = 21.4471(11) Å, V = 3189.4(3) $Å^3$ (Z = 8). The calculated density is 4.517 g/cm^3 using the empirical formula. Tazzoliite has no synthetic or natural analogue.

The structure of tazzoliite (Figure 3) consists of a framework of Nb(Ti)-octahedra and $A1O_8$(OH) polyhedra sharing apexes or edges, and Si-tetrahedra sharing apexes with Nb(Ti)-octahedra and $A1O_8$(OH) polyhedra. Tazzoliite is constituted by three different Nb(Ti)-octahedra, two of them are Nb dominant (site populations of $Nb_{0.86}Ti_{0.14}$ and $Nb_{0.76}Ti_{0.24}$, respectively) and one is Ti dominant (site population: $Ti_{0.80}Nb_{0.20}$). Ti-dominant octahedra form pairs sharing an edge along [010], which extend along [100] forming a double chain. Nb-dominant octahedra form a chain along [100], decorated by 4 Nb-dominant octahedra sharing apexes.

Chains of $A2O_8$ polyhedra extend along [100] and are surrounded by Nb-octahedra. $A2O_8$ polyhedra share edges with *Nb*1- and *Ti*3-octahedra.

We can consider also the presence of channels formed by six Nb-octahedra and two tetrahedra, or four $A1O_8$(OH) polyhedra, which alternate along [100]. The channels may be partially occupied by $[PO_2(OH)_2]$ in two mutually excluding positions, alternating with fully occupied $A3O_6$(OH) polyhedral pairs. The $[PO_2(OH)_2]$ anionic

group may show heterovalent substitution at the cation site (*P* site), which may be occupied by P, S or Si. This is the most complicated part of the structure: the partial occupation of the *P* sites rules the calculation of the end-member formulae. First of all, due to the mutual exclusive position of the *P* sites, it is implicit that a composition of tazzoliite with $[PO_2(OH)_2]_{x > 0.5}$ would never be possible. In addition, on the basis of charge requirements, S cannot be dominant on the site. The observed P-O distances are rather short, due to the difficulty of solving the complicated environment in the presence of $[PO_2(OH)_2]$ groups. Each P atom at the *P* sites is coordinated with two O9 sites and with two O10 sites. (OH) groups are present at the O9 site when the *P* site is occupied and at the O8 site when the *P* site is vacant. Moreover, the anion sites O8 and O10 are mutually exclusive. The same applies to H bonded to O9 [O8], only one alternative position can be occupied. Therefore, in terms of formula normalization, if the *P* site is vacant it means that there are 17 oxygen atoms per asymmetric unit plus one (OH) group at the O8 site, *i.e.* 18 anions. Fluorine may be also present at the O8 site. Therefore, (OH) + F must be 1 apfu. An occupation of the *P* site of *x* requires 2*x* additional oxygen atoms present at the O10 sites. Thus, the total amount of anions is 18 + 2*x*, being *x* the occupation of the *P* site [*i.e.*, P + S + (Si - 1)]. As previously stated, *x* cannot be > 0.5, and therefore the maximum quantity of anions is 19 apfu.

Raman spectroscopy

The Raman spectrum of tazzoliite (Figure 4) can be divided in three main regions: (1) 200–400 cm^{-1}; (2) 400–600 cm^{-1}; (3) 800–1200 cm^{-1}. The most intense peak at about 750 cm^{-1} needs to be discussed separately.

200–400 cm^{-1} range: this part of the spectrum is most likely due to vibrations between large cations (*e.g.*, Ba, Ca, Na, Sr) and oxygen atoms.

400–600 cm^{-1}: the Raman peaks in this region can be assigned to the Si-O-Si symmetric stretching vibrations and bending motions of Si-O-Si.

800–1200 cm^{-1}: finally, the high-frequency region Raman bands could be assigned to symmetric Si-O stretching motions of silicate units with one, two, three, or four non-bridging oxygen atoms. This region of the tazzoliite spectrum can also provide information about the $PO_2(OH)_2^{-1}$ group. Such group is very rare in minerals and not many Raman spectroscopy data are present in literature providing its vibrational modes. However, we found data on synthetic compounds like $M[PO_2(OH)_2)]\cdot 2H_2O$ with M = Mg, Mn, Fe, Co, Zn, Ni, Cd (Koleva and Heffenberger, 2007) for which the P-OH and P-O show two bands between 946 and 977 cm^{-1} and 1046 and 1070 cm^{-1}, respectively. Moreover, for synthetic compounds like NaH_2PO_4 and Na_2HPO_4, Dutta and Shieh (1985) report that the $PO_2(OH)_2^{-1}$ group shows two strong polarized bands at 880 cm^{-1} and 1060 cm^{-1} due to the P-OH and P-O stretches, respectively. Considering that the Raman spectrum of tazzoliite shows one peak at 869 cm^{-1}, two peaks between 961 and 981 cm^{-1} and a fourth peak at 1062 cm^{-1} (Figure 4) we are strongly confident about the presence of the $PO_2(OH)_2^{-1}$ group.

Relative to the most intense peak found at about 750 cm^{-1}, it has been reported in literature (Su *et al.*, 2000) that for synthetic nenadkevichite $[(Na,K)_2(Nb,Ti)_2[Si_4O_{12}](O,OH)_2\cdot 2H_2O]$, with a structure related to tazzoliite (see below), such a band has been assigned to Ti-O stretching vibrations of TiO_6 units. Similarly, for tazzoliite we could assign this band to Ti-O and Nb-O stretching vibrations of TiO_6 and NbO_6 units. Further evidence for this comes from the IR spectrum of komarovite $[(Ca,Mn)Nb_2[Si_2O_7](O,F)_3 \cdot 3.5H_2O]$ from Lovozero (most intense band at exactly 750 cm^{-1}; Pekov *et al.*, 2004). Concerning the OH group region, tazzoliite shows a very weak and broad peak at 3516 cm^{-1}, consistent with OH

stretching and confirming the crystal chemical formula proposed for tazzoliite. No evidence of H_2O bending at about 1600 cm^{-1} is present (even if present, the bending mode of H_2O at 1600 cm^{-1} would be too weak to be visible with respect to the already weak peak for OH stretching at 3516 cm^{-1}).

Site assignement

Cation sites

Tazzoliite has 3 large cation sites (*A*1, *A*2, *A*3), 3 octahedral sites (*Nb*1, *Nb*2 and *Ti*3) and one tetrahedral site (*Si*). Regarding the *Si* site, it shows an average bond distance <Si-O> = 1.647 Å, corresponding to a full occupation by Si.

Concerning the octahedral sites, the Nb-dominant octahedra (*Nb*1 and *Nb*2) show mean bond distances of 1.990 and 1.983 Å, respectively, that closely match the values found for kenopyrochlore [1.9855 Å – Bindi *et al.*, 2006; renamed from bariopyrochlore after the approval of the new scheme of nomenclature for the pyrochlore supergroup, approved by the CNMNC–IMA (Atencio et al., 2010)] and the value of 1.986 Å observed in hydropyrochlore [Ercit *et al.*, 1994; renamed after new scheme of nomenclature for the pyrochlore supergroup, approved by the CNMNC–IMA (Atencio et al., 2010)], having a *B*-site population very close to that observed in tazzoliite. On the other hand, the Ti-dominant octahedron shows a mean bond distance of 1.975 Å, which is consistent with the value obtained by considering the <Ti-O> bond of the pure $Y_2Ti_2O_7$ (1.953 Å – Becker and Will, 1970), and the sum of the Nb-O ionic radii (2.040 Å, respectively – Shannon, 1976). Indeed, taking into account the molar fractions of Ti and Nb in tazzoliite (*i.e.*, Ti = 0.80 and Nb = 0.20 *a.p.f.u.*) and the mean bond distances for the pure components, we obtain a value of 1.970 Å. If we consider the chemical analyses, site assignment must account for 0.07

apfu of Ta. The highest site scattering observed is at the *Nb*1 site. Therefore, we have assigned all the Ta at this site. The composition we obtain for the three octahedral sites is therefore $^{Nb1}(Nb_{1.64}Ti_{0.28}Ta_{0.07}Zr_{0.01})$ $^{Nb2}(Nb_{0.78}Ti_{0.22})$ $^{Ti3}(Ti_{1.55}Nb_{0.45})$, which correspond to the observed and calculated site scattering values of 76.78 vs. 78.91, 36.44 vs. 36.82, 51.6 vs. 52.55 e- pfu, respectively.

The large cation sites have different coordination environments and site populations. The *A*1 site is coordinated by 7 oxygen atoms and one (OH) group, plus a long bond to the partially occupied O10 site. Site occupancy refinement shows that *A*1 site has 53.48 electrons per site (eps). As this is the largest cation site in the structure we assign all the Ba to this site. Chemical analyses report 1.93 apfu and there are 2 *A*1 sites pfu. This corresponds to 0.965 atoms of Ba per *A*1 site and the remaining can be assigned as Na, which makes a calculated site scattering of 54.43 eps. The *A*2 site is a highly regular polyhedron and has refined site occupancy of 29 eps. There is one *A*2 site pfu. This site is the smaller site and the lower observed site scattering with respect to *A*1 site lead us to assign mostly smaller species, i.e. Ca, Fe^{2+} and Sr to this site. This makes $Sr_{0.53}Ca_{0.38}Fe^{2+}_{0.09}$, which corresponds to a calculated site scattering of 30.08 eps and a mean charge of 2. This is just slightly higher than the observed value. Regarding the *A*3 site, it shows 7-fold coordination. Its observed site scattering is 17.84 eps requiring thus the lower scattering species at this site. We have left 0.82 apfu of Ca, and 0.18 Na apfu, which makes a calculated site-occupancy of 18.38 eps, just slightly higher than the observed value. In overall, the composition of cation sites is

$^{A1}(Ba_{1.93}Na_{0.06})^{A2}(Sr_{0.53}Ca_{0.38}Fe^{2+}_{0.09})^{A3}(Ca_{0.82}Na_{0.18})^{Nb1}(Nb_{1.64}Ti_{0.28}Ta_{0.07}Zr_{0.01})^{Nb2}(Nb_{0.78}Ti_{0.22})^{Ti3}(Ti_{1.55}Nb_{0.45})Si$. Ideally, we have $Ba_2SrCaNb_3Ti_2Si$ with a charge of +35.

Anion sites.

There are 7 anion sites fully occupied by oxygen atoms in the structure of tazzoliite, which account for 17 apfu. There are 3 anion sites which are related to the $[PO_2(OH)_2]$ anionic group environment, O8, O9 and O10. The *P* site is coordinated by 2 (OH) groups at the O9 anion site and two oxygen atoms at the O10 site, and can be occupied at maximum at 50% as the two 8*g* positions are mutually exclusive. This also implies that only half of the 16*o* positions of the O10 sites can be occupied. The observed excess site occupancy of 0.58 at O10 (Table 4) should be ascribed to the difficulty to refine the positional disorder. During the refinement we have not constrained the site occupancies at the O9 and O10 sites, nor the isotropic displacement parameters. The dihydrogen phosphate group will therefore alternate in two positions along [100], otherwise would share one edge, with a very short P-P distance. When the *P* site is vacant, the O8 site is occupied by (OH) groups or F and both the O9 and O10 sites are vacant. Thus, the *A*1 polyhedron turns seven-fold coordinated, while the *A*3 polyhedron maintains its coordination number but turns smaller, as A3-O8 is shorter than A3-O10, in agreement with a full occupation by Ca.

Therefore, the anion composition is $O_{17} + [PO_2(OH)_2]_{0.5}$ with a charge of -34.5 or O_{17} + (OH) with a charge of -35. The latter matches the charge of the ideal cationic composition. The former needs a reduction of charge of +0.5, which is accomplished by substitution of a divalent cation by up to 0.5 apfu of a monavalent cation, for example Na.

Therefore the ideal composition of this structural type will range from $Ba_2SrCaNb_3Ti_2Si\ O_{17}(OH)$ to $Ba_2SrCa_{0.5}Na_{0.5}Nb_3Ti_2SiO_{17}[PO_2(OH)_2]_{0.5}$. This would lead to two ideal compositions. The mineral composition we have studied has [P+S+(Si-1)] > 0.25 and thus we define tazzoliite as $Ba_2CaSr_{0.5}Na_{0.5}Nb_3Ti_2SiO_{17}$

$[PO_2(OH)_2]_{0.5}$, which requires P_2O_5 3.24, Nb_2O_5 36.47, SiO_2 5.50, TiO_2 14.62, BaO 28.06, CaO 5.13, SrO 4.74, Na_2O 1.42, H_2O 0.82, Total 100.00 wt%, and a mineral with $Ba_2SrCaNb_3Ti_2Si\ O_{17}(OH)$ would correspond to a new species.

Relation to other structures

Tazzoliite is related to the pyrochlore structure (Atencio et al., 2010) with the addition of a slab of $SiTiO_3[PO_2(OH)_2]_{0.5}$ every 0.5 *b* translation parallel to [110] of pyrochlore (Figure 3). Other pyrochlore-related structures have been described by Ferraris *et al.* (2008) although they have alternate one [K-rich nenadkevichite $(Na,K)(Nb,Ti)_2[Si_4O_{12}](O,OH)_2 \cdot 1.6H_2O$, Rastsvetayeva *et al.*, 1994], two [fersmanite $(Ca_{5.49}Na_{2.37}Sr_{0.08}Fe_{0.06})(Nb_{1.61}Ti_{2.39})(Si_2O_7)_2O_8F_3$, Sokolova *et al.*, 2002], or three [Na-rich komarovite $Na_{5.5}Ca_{0.8}La_{0.2}Ti_{0.5}Nb_{5.5}Si_4O_{26}F_2 \cdot H_2O$, Balič Žunič *et al.*, 2002] octahedra-thick (100)-pyrochlore slabs with (SiO_4) groups with different degrees of polymerization (four-membered rings being the most frequent unit) (Figure 5). Tazzoliite thus represents a novel type of pyrochlore-related structure, which includes further anionic groups other than (SiO_4). One of the anionic groups coordinates with (OH) groups. The dominant cation at the centre of the (MO_4) anionic group is phosphorous. The presence of dihydrogen phosphate groups has been observed in girvasite, $(NaCa_2Mg_3(PO_4)_2[PO_2(OH)_2](CO_3)(OH)_2 \cdot 4H_2O$ (Sokolova *et al.*, 1990).

Acknowledgments

We are really delighted to contribute to this issue dedicated to Mark Welch, a well-known European mineralogical crystallographer. Most of us collaborated with him during the last years and Mark gave, as usual, a very remarkable contribution. His

longstanding studies on hydrous silicates are especially noteworthy, and they undoubtedly represent a solid basis for all the scientific community.

We would like to thank Bruno Fassina for providing us tazzoliite. We also thank Mr. Fassina for the photo of tazzoliite shown in Figure 1. L. Tauro and E. Masiero are thanked for sample preparation and R. Carampin for the microprobe analysis. The work was supported by "Progetto d'Ateneo 2006 from University of Padova" to F. Nestola. We thank Associate Editor Diego Gatta, Stuart Mills and one anonymous referee for constructive comments, which helped to improve the manuscript.

References

Atencio D., Andrade M.B., Christy A.G., Giere R., Kartashov P.M. (2010) The pyrochlore supergroup of minerals: nomenclature. *Canadian Mineralogist,* **48**, 673-698.

Astolfi, F. Colombara F. (2003) *La geologia dei Colli Euganei.* Edizioni Canova. Treviso.

Balič Žunič, T., Petersen, O.V., Bernhardt, H.-J. and Michelssen, H.I. (2002) The crystal structure and mineralogical description of a Na-dominant komarovite from the Ilimaussaq alkaline complex. South Greenland. *Neues Jahrbuch für Mineralogie,* Monatshefte, 2002, 497–514.

Becker von, W.J. and Will, G. (1970) Röntgen- und Neutronenbeugungsuntersuchungen an $Y_2Ti_2O_7$. *Zeitschrift für Kristallographie*, **131**, 278–288.

Bindi, L., Petříček, V., Withers, R.L., Zoppi, M. and Bonazzi, P. (2006) Novel high-temperature commensurate superstructure in natural bariopyrochlore: a

structural study by means of a multiphase crystal structure refinement. *Journal of Solid State Chemistry*, **179**, 716–725.

Dal Piaz, G. (1935) La costituzione geologia dei Colli Euganei. *Atti e Memorie dell'Accademia Patavina di Scienze, Lettere ed Arti*, **51**, 11-19.

Downs, R.T., Bartelmehs, K.L., Gibbs, G.V., and Boisen, M.B.Jr. (1993) Interactive software for calculating and displaying X-ray or neutron powder diffractometer patterns of crystalline materials. *American Mineralogist*, **78**, 1104–1107.

Dutta, P.K., and Shieh, D.C (1985) Raman spectral study of the composition of basic silicate solutions. *Applied Spectroscopy*, **39**, 343-346.

Ercit, T.S., Hawthorne, F.C. and Černý, P. (1994) The structural chemistry of kalipyrochlore, a "hydropyrochlore". *Canadian Mineralogist*, **32**, 417–420.

Ferraris, G., Mackovicky, E. and Merlino, S. (2008) *Crystallography of Modular Materials*. Oxford University Press, New York.

Koleva, V., and Effenberger, H. (2007) Crystal chemistry of $M[PO_2(OH)_2)]\cdot 2H_2O$ compounds (M = Mg, Mn, Fe, Co, Ni, Zn, Cd): structural investigation of the Ni, Zn and Cd salts. *Journal of Solid State Chemistry*, **180**, 956–967

Mandarino, J.A. (1976) The Gladstone-Dale relationship-part I: derivation of new constants. *Canadian Mineralogist*, **14**, 498–502.

Palatinus L., Chapuis G. (2007) Superflip - a computer program for the solution of crystal structures by charge flipping in arbitrary dimensions. *Journal of Applied Crystallography*, **40**, 786–790.

Pekov, I.V., Azarova, Y.V. and Chukanov, N. (2004) New data on komarovite series minerals. *New Data on Minerals*, **39**, 5–13.

346 Rastsvetayeva, R.K., Tamezyan, R.A., Puscharovsky, D.Yu. and Nadeshina, T.M.
347 (1994) Crystal structure and micro-twinning of K-rich nenadkevichite.
348 *European Journal of Mineralogy*, **6**, 503–509.
349 Shannon, R.D. (1976) Revised effective ionic radii and systematic studies of
350 interatomic distances in halides and chalcogenides. *Acta Crystallographica*,
351 **A32**, 751–767.
352 Sheldrick, G.M. (2008) A short history of SHELX. *Acta Crystallographica*, **A64**,
353 112-122.
354 Sokolova Y.V. and Yegorov-Tismenko Y.K. (1990) Crystal structure of girvasite.
355 *Doklady Akadamii Nauk SSSR*, **331**, 1372–1376.
356 Sokolova, E., Hawthorne, F.C. and Khomyakov, A.P. (2002) The crystal chemistry of
357 fersmanite, $Ca_4(Na,Ca)_4(Ti,Nb)_4(Si_2O_7)_2O_8F_3$. *Canadian Mineralogist*, **40**,
358 1421–1428.
359 Stark, M. (1936) Kalksilikatgesteine bei Galzignano in den Euganeen. *Neues*
360 *Jahrbuch für Mineralogie, Geologie und Paläontologie*, **71**, 342-361.
361 Su, Y., Lou Balmer, M. and Bunker, B.C. (2000) Raman spectroscopic studies of
362 silicotitanates. *Journal of Physical Chemistry B*, **104**, 8160–8169.
363

Table and figure captions

Table 1. Microprobe analyses for tazzoliite based on 7 analysis points.

Table 2. Crystal data for tazzoliite.

Table 3. X-ray powder diffraction patterns for tazzoliite.

Table 4. Atom coordinates and equivalent isotropic displacement parameters ($Å^2$) for tazzoliite. *U*(eq) is defined as one third of the trace of the orthogonalized U_{ij} tensor.

Table 5. Selected geometric parameters (Å).

Figure 1. Geological map of the Monte delle Basse zone where Tazzoliite was found (modified from Astolfi and Colombara, 2003).

Figure 2. Appearance of tazzoliite under a conventional stereoscopic microscope (photo by Bruno Fassina).

Figure 3. Crystal structure of tazzoliite and its relationships with pyrochlore structure. Light yellow polyhedra are Nb/Ti sites; orange tetrahedra are Si sites; yellow tetrahedra (P,Si,S) are partially occupied sites; violet spheres indicate *A*1 sites; grey spheres are Sr and Ca dominant sites (*A*2 and *A*3); red spheres are O atoms; small white spheres are H atoms; green spheres are F atoms.

Figure 4. Raman spectrum of tazzoliite collected between 150 and 3700 cm^{-1}. In figure 3a and 3b the ranges between 150 and 2000 cm^{-1} and 3000 and 3700 cm^{-1} are shown, respectively.

Figure 5. Relationships among known pyrochlore-like structures.

Table 1

Constituent	wt%	Range	SD	Probe Standard (analysing crystals)
SO_3	0.51	0.36-0.66	0.10	$BaSO_4$ (PET)
Nb_2O_5	34.51	33.53-35.38	0.63	Pure metal for Nb (PET)
Ta_2O_5	0.89	0.66-1.16	0.16	Pure metal for Ta (LiF)
V_2O_3	0.05	0.00-0.11	0.04	Vanadinite (LiF)
P_2O_5	0.85	0.85-0.85		Apatite (TAP)
SiO_2	6.10	5.74-6.31	0.19	Diopside (Si TAP; Ca PET)
TiO_2	14.77	14.42-15.09	0.27	$MnTiO_3$ (PET)
SnO_2	0.04	0.00-0.09	0.03	SnO_2 (PET)
ZrO_2	0.11	0.07-0.21-	0.10	Synthetic zircon (PET)
FeO	0.63	0.55-0.66	0.04	Fe_2O_3 (LiF)
MnO	0.01	0.00-0.03	0.17	$MnTiO_3$ (LiF)
CaO	6.07	5.67-6.60	0.02	Diopside (PET)
BaO	26.75	26.31-27.28	0.39	$BaSO_4$ (LiF)
SrO	4.92	4.18-5.72	0.48	Celestine (PET)
Na_2O	0.70	0.64-0.77	0.05	Amelia (TAP)
H_2O*	0.74	0.64-0.73	0.05	
F	0.15	0.00-0.37	0.16	Fluorite (TAP)
O = F	-0.06			
Total	**97.74**			

*From crystal structure stoichiometry.

Table 2

Space group	*Fmmm*
a (Å)	7.4105(4)
b	20.0675(11)
c	21.4471(11)
V (Å^3)	3189.4(3)
Z	4
Absorption coefficient (mm^{-1})	8.864
F(000)	3941
$D_{calc.}$ (g/cm^3)	4.489
Crystal size (mm)	0.015 x 0.04 x 0.10
Radiation/filter	Mo*K*α/graphite
2θ-range for data collection (°)	1.90 to 30.00°.
R(int) (%)	5.40
Reflections collected	12200
Index ranges	$-10 \leq h \leq 10$ $-28 \leq k \leq 28$, $-30 \leq l \leq 30$
Independent reflections	1312
$F_o > 4\sigma F$	1300
Refinement method	Full-matrix least squares on F^2, fixed weights proportional to $1/\sigma F_o^2$
No. of refined parameters	95
Final $R_{(obs)}$ (%)[$F_o > 4\sigma F$]	6.25
R_1	6.33
wR_2	15.81
Goodness of fit on F^2	1.246

421

422 **Table 3**

hkl	d_{obs} (Å)*	I_{rel}	d_{calc} (Å)**	I_{rel}
0 0 2			10.724	2
0 2 0			10.034	36
0 2 2	7.3	15	7.327	15
0 0 4			5.362	3
0 4 0	5.0	15	5.017	13
2 0 0	3.71	10	3.705	11
0 4 4	**3.66**	**60**	3.663	47
1 1 5			3.650	8
2 0 2	3.49	20	3.502	10
1 5 1			3.482	17
2 2 2	3.31	10	3.307	8
1 3 5	3.25	5	3.246	5
1 5 3	**3.16**	**30**	3.165	29
2 0 4	**3.05**	**100**	3.048	100
2 4 0	**2.979**	**25**	2.981	25
2 2 4	2.918	10	2.917	11
0 4 6	2.910	15	2.911	12
2 4 2	2.872	10	2.872	10
0 6 4	**2.835**	**50**	2.838	47
1 1 7	2.801	10	2.804	8
1 5 5	2.723	20	2.725	18
0 0 8	2.678	20	2.681	19
1 7 1	2.652	5	2.653	5
1 3 7	2.606	5	2.607	3
2 4 4			2.605	5
0 8 0	2.510	5	2.508	3
2 6 0	2.483	15	2.483	12
2 4 6			2.289	3
1 7 5	2.270	15	2.269	14
1 1 9			2.254	3
2 0 8			2.172	3
1 3 9			2.148	3
1 9 1	2.126	10	2.125	8
0 6 8			2.092	3
1 9 3			2.046	4
3 5 3	2.015	10	2.018	8
2 4 8	1.995	20	1.993	17
0 4 10			1.972	2
2 8 4			1.937	4
3 1 7	1.913	15	1.914	6
1 9 5			1.911	9
3 5 5	1.889	5	1.889	6
3 7 1			1.864	3
2 0 10	**1.854**	**25**	1.856	3
4 0 0			1.853	17
3 3 7			1.848	3

2 6 8	**1.822**	**25**	1.822	22423
1 3 11	1.813	5	1.815	6
2 8 6	1.795	5	1.796	6
1 7 9			1.779	2
1 11 1	1.765	10	1.765	8
2 4 10	1.741	10	1.741	8
1 11 3			1.719	2
2 10 4			1.676	4
4 4 4	1.652	10	1.653	6
3 9 1			1.650	3
1 11 5	1.636	5	1.637	4
0 8 10	1.629	5	1.630	4
2 6 10			1.623	3
2 0 12	1.610	5	1.610	4
0 12 4			1.596	2
0 6 12	1.575	5	1.576	5
4 4 6			1.563	3
4 6 4	1.552	10	1.551	13
3 9 5			1.544	2
4 0 8	1.523	10	1.524	8
3 3 11			1.492	3
2 12 4			1.466	2
3 11 1			1.464	2
3 11 3			1.438	2
1 11 9			1.422	2
2 12 6	1.401	5	1.402	4
1 1 15			1.401	2

*: Observed powder pattern for obtained with a fully indexed 114.6 mm Gandolfi camera (Ni-filtered Cu*K*α radiation).**: Calculated pattern and indexing on the basis of *a* = 7.4105(4) Å, *b* = 20.0675(11) Å, *c* = 21.4471(11) Å, and with the atom coordinates and occupancies reported in Table 4. Intensities were calculated using XPOW software (Downs *et al*., 1993).

Table 4

Atom	Wyck.	Occ.	*x*/*a*	*y*/*b*	*z*/*c*	Ueq
*A*1 (Ba)	16*m*	0.93 Ba + 0.07 Ca	0	0.12852(5)	0.10553(4)	0.013(1)
*A*2 (Ca)	8*f*	0.75 Ca + 0.25 Ba	¼	¼	¼	0.010(1)
*A*3 (Ca)	8*h*	0.76 Ca + 0.24 Na	- ½	0.0963(3)	0	0.026(2)
*Nb*1	16*m*	0.86 Nb + 0.14 Ti	- ½	0.17122(6)	0.13211(6)	0.009(1)
*Nb*2	8*e*	0.76 Nb + 0.24 Ti	¼	¼	0	0.010(1)
Ti3	16*k*	0.80 Ti + 0.20 Nb	¼	0.07937(10)	¼	0.012(1)
Si	8*i*	1.00	½	0	0.1470(2)	0.008(1)
O1	8*h*	1.00	0	0.2139(7)	0	0.008(2)
O2	32*p*	1.00	0.3040(9)	0.1426(3)	0.1887(3)	0.010(1)
O3	16*m*	1.00	0	0.2469(5)	0.1706(4)	0.007(2)
O4	16*n*	1.00	0.3188(13)	0	0.1927(4)	0.008(2)
O5	32*p*	1.00	0.3180(9)	0.1841(3)	0.0646(3)	0.011(1)
O6	16*m*	1.00	- ½	0.0680(5)	0.1053(5)	0.013(2)
O7	16*m*	1.00	0	0.0723(5)	0.2180(5)	0.011(2)
O8	8*g*	0.43	-0.340(5)	0	0	0.018(10)
P	8*g*	0.28	0.066(4)	0	0	0.038(9)
O9	8*i*	0.82	0	0	0.065(2)	0.071(15)
H9	16*n*	0.43	0.11200	0	0.09000	0.0850
O10	16*o*	0.58	0.177(4)	0.0582(13)	0	0.036(8)

Table 5

Nb1—O3	1.839(10)	A1—O7	2.663(11)
Nb1—O2 x2	1.978(7)	A1—O9	2.722(14)
Nb1—O5 x2	1.996(7)	A1—O5 x2	2.751(7)
Nb1—O6	2.15(1)	A1—O3	2.755(10)
<Nb1—O>	1.990	A1—O1	2.839(9)
Nb2—O5 x4	1.980(6)	A1—O2 x2	2.887(7)
Nb2—O1 x2	1.989(5)	A1—O10	2.972(18)
<Nb2—O>	1.983	<A1—O>	2.830
Ti3—O2 x2	1.870(6)	A2—O3 x4	2.517(6)
Ti3—O7 x2	1.981(4)	A2—O2 x4	2.556(6)
Ti3—O4 x2	2.075(6)	<A2—O>	2.537
<Ti3—O>	1.975	A3—O8	2.267(20)
Si—O6^{ii} x2	1.632(11)	A3—O6 x2	2.329(11)
Si—O4 x2	1.662(10)	A3—O10^{i}	2.513(29)
<Si—O>	1.647	A3^{ii}—O5 x4	2.616(8)
P—O10 x2	1.429(32)	<A3—O>*	2.484
P—O9 x2	1.477(42)	<A3—O>**	2.519
<P—O>	1.453	O9—H9	0.988(23)
		O8—O10	1.68(4)

Symmetry codes are (i): -1+*x*, *y*, *z*; (ii): 1+*x*, *y*, *z*; (iii): -*x*, -*y*, *z*; (iv): -2+*x*, *y*, *z*; (v): 1-*x*, -*y*, *z*. *Average including O8 and excluding O10; ** average including O10 and excluding O8.

FIGURE 1

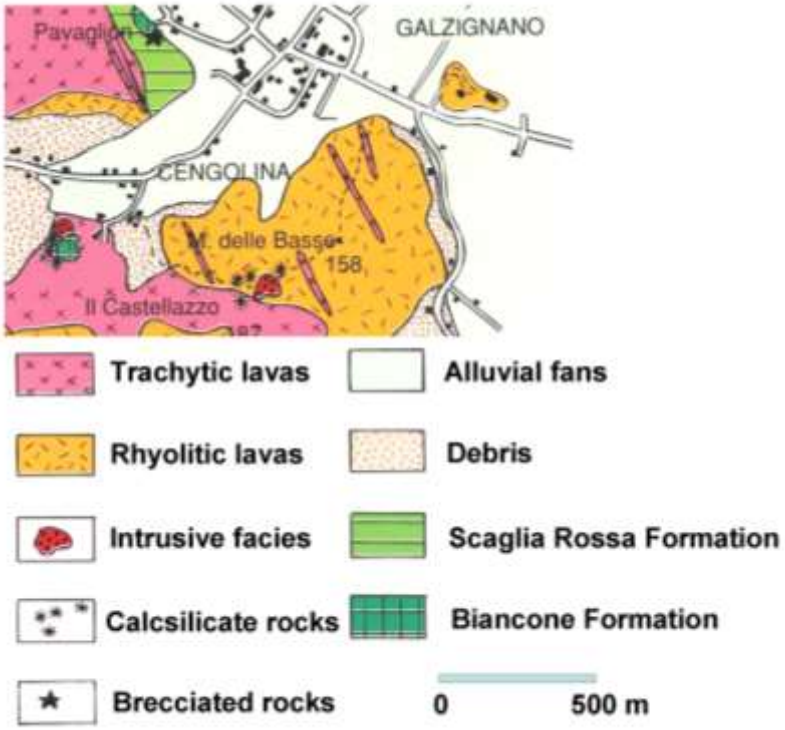

FIGURE 2

FIGURE 3

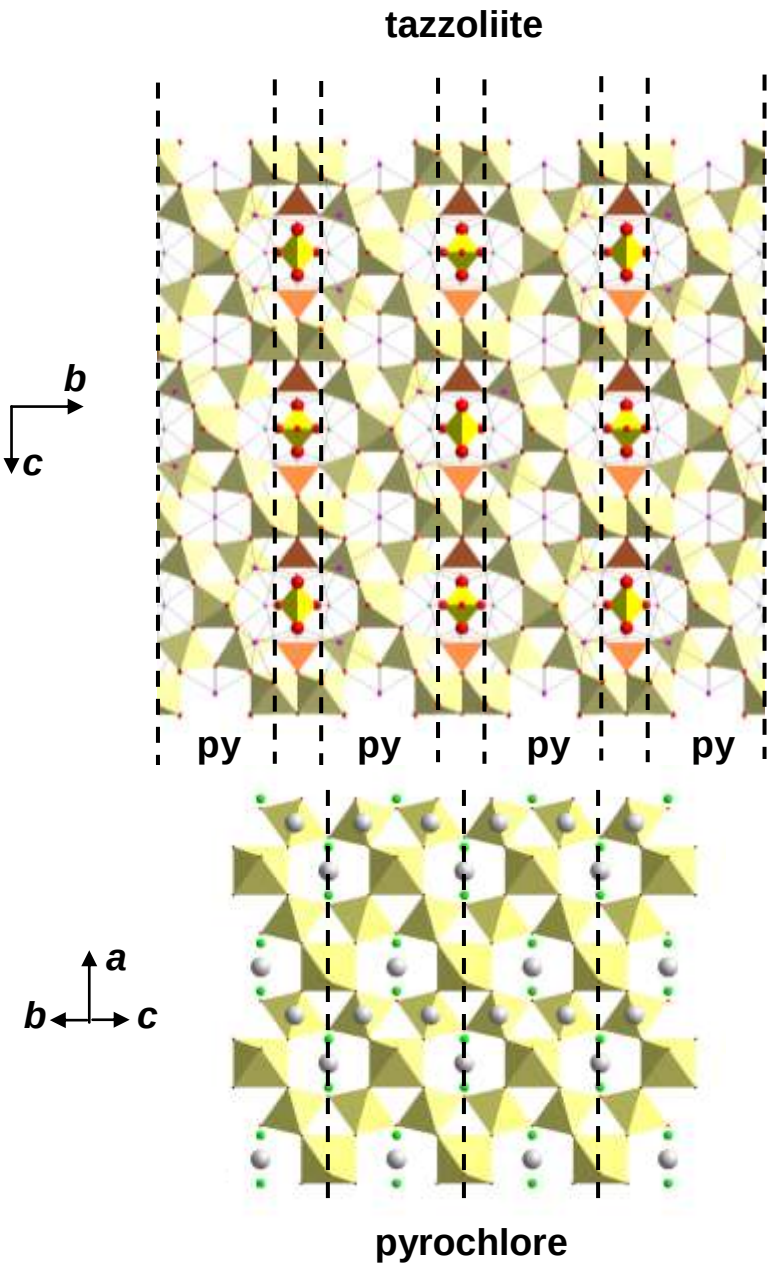

FIGURE 4

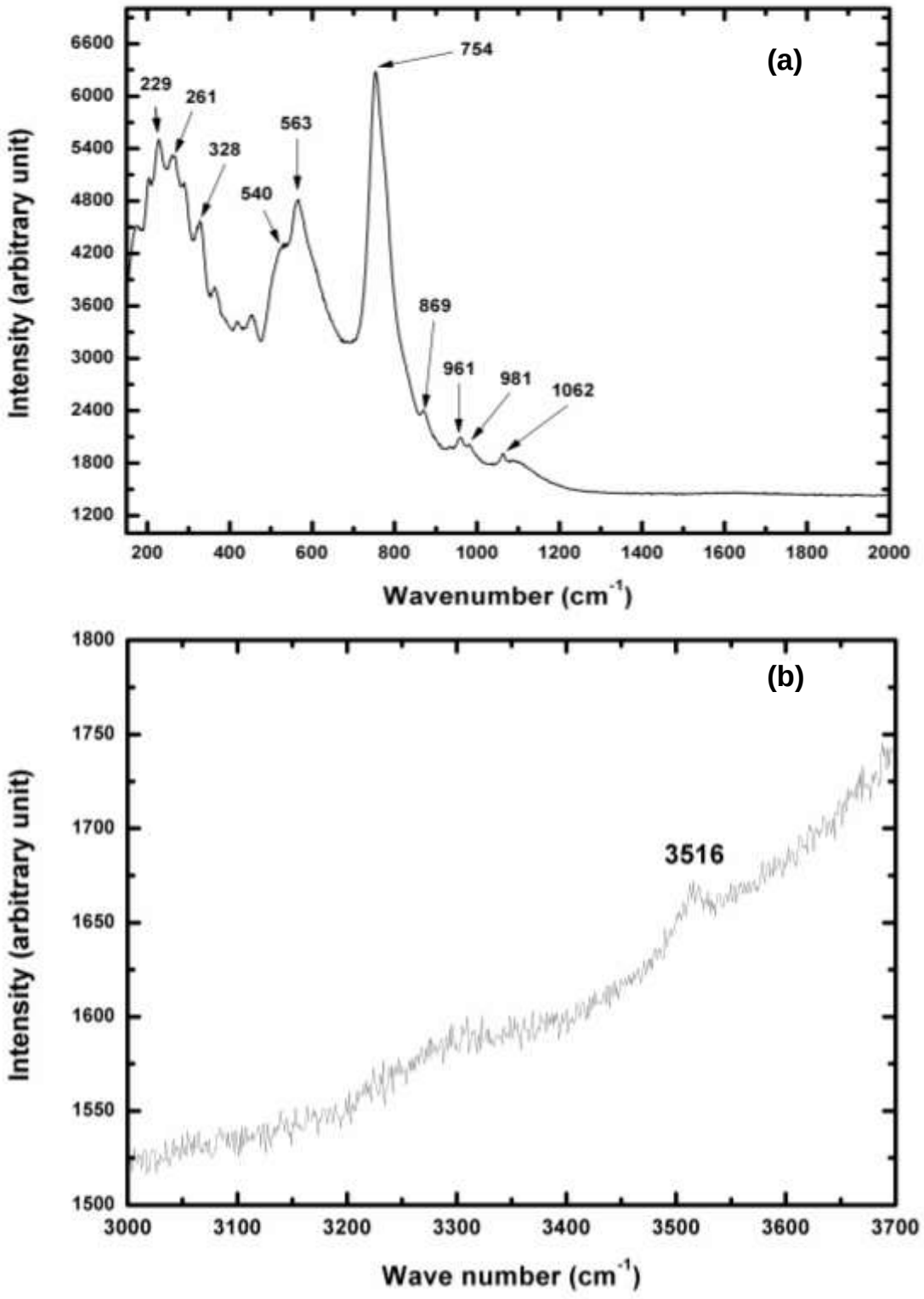
(a)
754
229
261
563
328
540
869
961
981
1062
Intensity (arbitrary unit)
Wavenumber (cm-1)
(b)
3516
Intensity (arbitrary unit)
Wave number (cm-1)

FIGURE 5

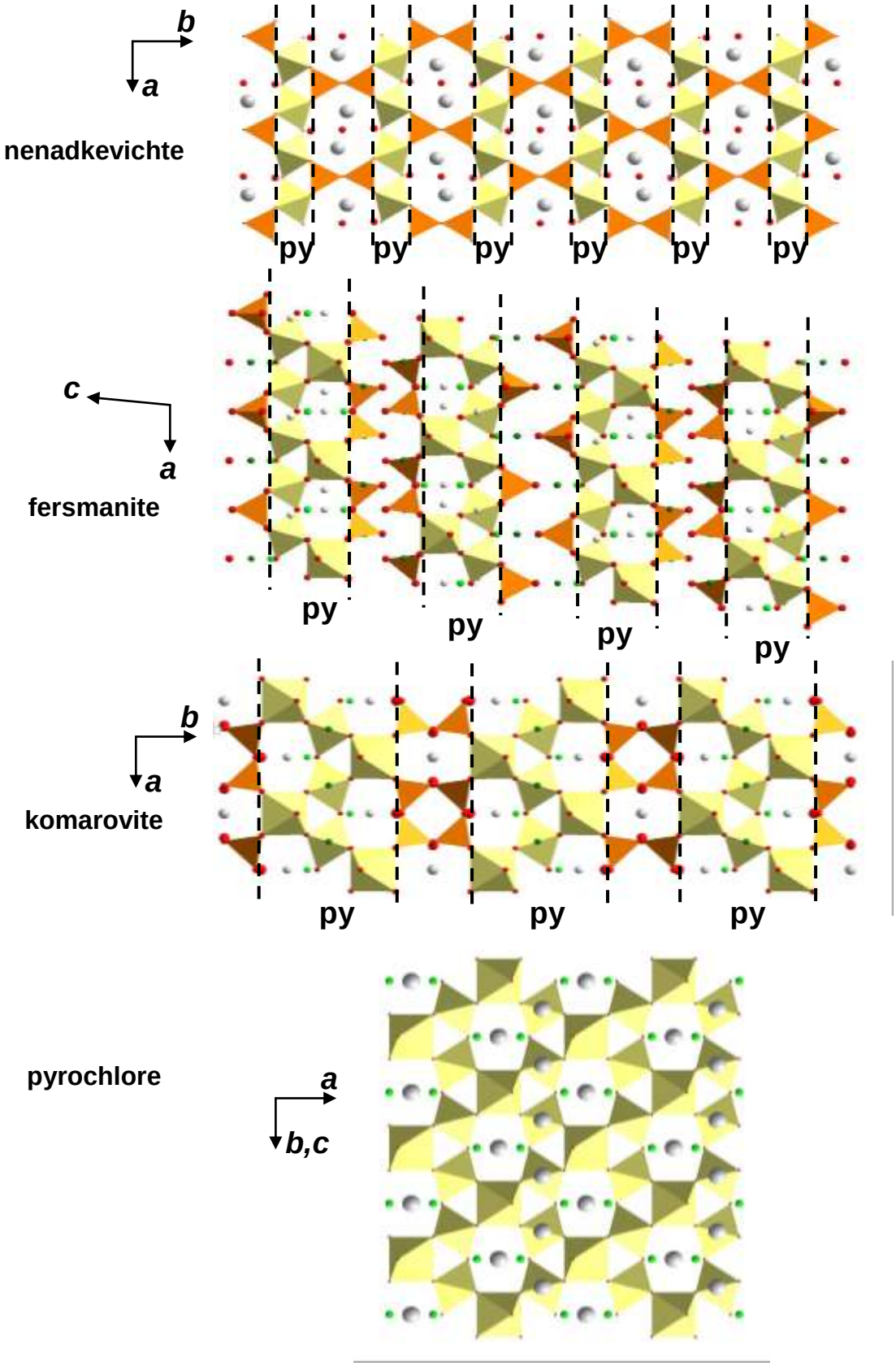
b
a
nenadkevichte
py
py
py
py
py
py
c
a
fersmanite
py
py
py
py
b
a
komarovite
py
py
py
pyrochlore
a
b,c